



Research article

The anti-hyperlipidemia effect of *Atractylodes macrocephala* Rhizome increased HDL via reverse cholesterol transfer

Bo Li^{a,c,d,1}, Xian-fang Chen^{a,1}, Han-song Wu^{a,1}, Jie Su^{b,1}, Yan-yan Ding^a, Ze-hua Zhang^a, Mei Rong^a, Ying-jie Dong^a, Xinglishang He^a, Lin-zi Li^a, Gui-yuan Lv^{b,**}, Su-hong Chen^{a,c,d,*}

^a Collaborative Innovation Center of Yangtze River Delta Region Green Pharmaceuticals, Zhejiang University of Technology, Hangzhou, Zhejiang, 310014, PR China

^b College of Pharmaceutical Science, Zhejiang Chinese Medical University, Hangzhou, Zhejiang, 310053, PR China

^c Zhejiang Provincial Key Laboratory of TCM for Innovative R & D and Digital Intelligent Manufacturing of TCM Great Health Products, Huzhou, Zhejiang Province, 313200, PR China

^d Zhejiang Synergetic Traditional Chinese Medicine Research and Development Co., Ltd, Huzhou, Zhejiang, 313200, PR China

ARTICLE INFO

Keywords:

Hyperlipidemia

HDL

Atractylodes macrocephala Rhizome (AM)

Network pharmacology

Reverse cholesterol transport (RCT)

ABSTRACT

Aim: *Atractylodes macrocephala* Rhizome (AM) has been used to treat hyperlipidemia for centuries, but its functional components and mechanisms are not clear. This research aimed to investigate the active components in AM and the mechanisms that underlie its anti-hyperlipidemia effect.

Methods: SD rats were fed a high-sucrose high-fat diet in conjunction with alcohol (HSHFDAC) along with different AM extracts (AMW, AMO, AME, and AMP) for 4 weeks. AM's active components were analyzed using multiple databases, and their mechanisms were explored through network pharmacology. The relationship between AM's effect of enhancing serum HDL-c and regulating the expression of reverse cholesterol transport (RCT)-related proteins (Apo-A1, LCAT, and SR-BI) was further validated in the HSHFDAC-induced hyperlipidemic rats. The kidney and liver functions of the rats were measured to evaluate the safety of AM.

Results: AMO, mainly comprised of volatile and liposoluble components, contributed the most significant anti-hyperlipidemia effect among the four extracts obtained from AM, significantly

Abbreviations: AM, *Atractylodes macrocephala* Rhizome; AMW, Water extract of AM; AMO, Petroleum ether extract of AM; AME, AM non-polysaccharides; AMP, AM polysaccharides; Apo-A1, Apolipoprotein A1; ALT, Alanine transaminase; AST, Aspartate transaminase; Akt1, RAC-alpha serine/threonine-protein kinase; AMPK, Adenosine 5'-monophosphate-activated protein kinase; ABCA1, ATP-binding-cassette A1; BUN, Blood urea nitrogen; Cr, Creatine; C-T, Compounds-Target; C-T-P, Compounds-targets-pathways; DIBP, Diisobutyl phthalate; ELISA, Enzyme linked immunosorbent assay; EGFR, Epidermal growth factor receptor; FoxO, Forkhead box O; GO, Gene ontology; HSHFDAC, High-sucrose high-fat diet in conjunction with alcohol; HE, Hematoxylin and eosin; HDL, High-density lipoprotein; HDL-c, High-density lipoprotein cholesterol; IL, Interleukin; IHC, Immunohistochemistry; KEGG, Kyoto Encyclopedia of Genes and Genomes; LDL-c, Low-density lipoprotein cholesterol; LDL, Low-density lipoprotein; LCAT, Lecithin cholesterol acyl transferase; mTOR, Mechanistic target of rapamycin; mTORC1, Mechanistic target of rapamycin complex 1; PPI, Protein-protein interaction; PPARγ, Peroxisome proliferator-activated receptor gamma; PI3K, Phosphatidylinositol 3-kinase; RCT, Reverse cholesterol transport; SR-BI, Scavenger receptor class B type I; TCM, Traditional Chinese Medicine; TCMS, Traditional Chinese Medicine Systems Pharmacology; TC, Total cholesterol; TG, Triacylglycerols; TNF, Tumor necrosis factor; VEGFA, Vascular endothelial growth factor A.

* Corresponding author. Collaborative Innovation Center of Yangtze River Delta Region Green Pharmaceuticals, Zhejiang University of Technology, Hangzhou, Zhejiang, 310014, PR China.

** Corresponding author.

E-mail addresses: zjtcmlgy@163.com (G.-y. Lv), chensuhong@zjut.edu.cn (S.-h. Chen).

¹ These authors contributed equally to this work and should be considered co-first authors.

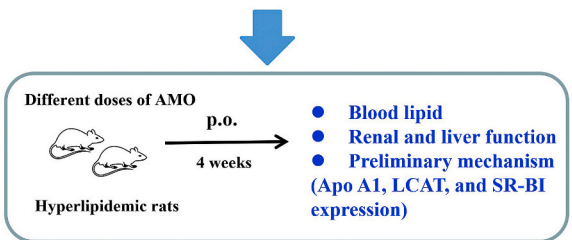
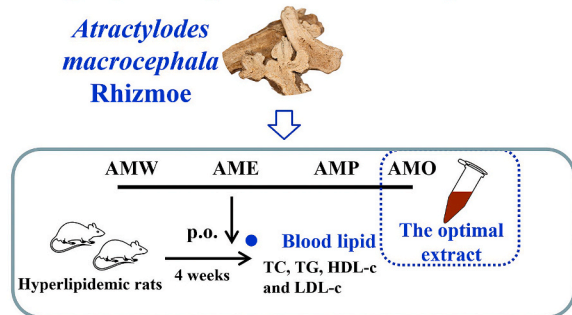
<https://doi.org/10.1016/j.heliyon.2024.e28019>

Received 25 June 2023; Received in revised form 8 March 2024; Accepted 11 March 2024

Available online 19 March 2024

2405-8440/© 2024 The Authors. Published by Elsevier Ltd. This is an open access article under the CC BY-NC license (<http://creativecommons.org/licenses/by-nc/4.0/>).

1. Hypolipidemic Effect Evaluated and Compared



3. Hypolipidemic Effect and Mechanism Verified

2. The Network Pharmacy Analysised

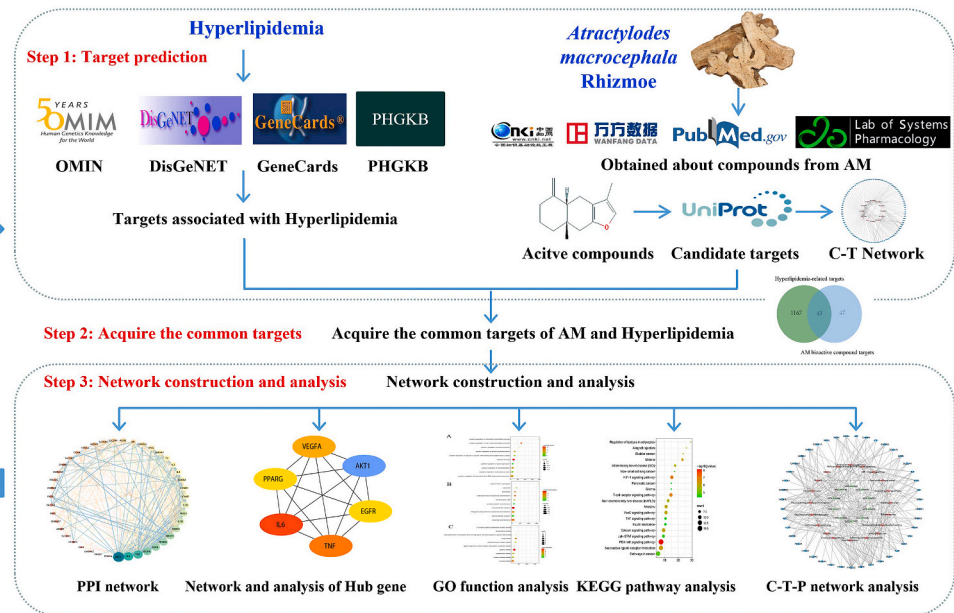


Fig. 1. Workflow of the Systems Pharmacology Study for AM treatment of hyperlipidemia.

improving the blood lipid profile. Network pharmacology analysis also suggested that volatile and liposoluble components, comprise AM's main active components and they might act on signaling pathways associated with elevated HDL-c. Validation experiments found that AMO substantially and dose-dependently increased HDL-c levels, upregulated the expression of Apo-A1, SR-BI, and LCAT, improved the pathological changes in the kidney and liver, and significantly reduced the serum creatinine levels in rats with hyperlipidemia.

Conclusion: The main anti-hyperlipidemia active components of AM are its volatile and liposoluble components, which may enhance serum HDL-c by increasing the expression of the RCT-related proteins Apo-A1, LCAT, and SR-BI.

1. Introduction

Hyperlipidemia has a considerable worldwide prevalence. It is marked by increased circulating levels of total cholesterol (TC), low-density lipoprotein (LDL) cholesterol (LDL-c), and triacylglycerol (TG), and may also involve a decreased concentration in the blood of high-density lipoprotein (HDL) cholesterol (HDL-c) [1]. According to a comprehensive adult survey conducted in China, 34.0% of Chinese individuals have dyslipidemia overall, representing a significant increase compared with the previous decade [2]. Hyperlipidemia is considered a danger measure for the formation of peripheral artery diseases, atherosclerosis, and coronary artery disease [3]. Lowering LDL-c has been shown to safely lead to additional decreases in the rate of coronary revascularizations, cardiovascular death, strokes, and myocardial infarction [4]. However, even in cases where serum LDL-c reaches a normal level, 30% of patients will still present with coronary heart disease [5], which may be related to a low HDL-c level [6,7]. Many drugs have been approved to treat hyperlipidemia, yet their efficacy is often affected due to side effects, individual variability, liver toxicity, and kidney toxicity [8]. The demand for the treatment of hyperlipidemia is significant, especially for methods that up-regulate the HDL-c level in a safe and systematic way.

Traditional Chinese medicine (TCM) has great potential for development in the treatment of hyperlipidemia due to its multi-target, multi-pathway, and multi-component modulating characteristics [9]. *Atractylodes macrocephala* Rhizome (AM, Bai Zhu in Chinese) is a well-known TCM that was first reported in the Chinese medical book authored by "Shen Nong Ben Cao Jing" approximately 2000 years ago. It has long been widely used in China as a digestive, a diuretic, and an antihidrotic medicine. AM is also included in many ancient Chinese prescriptions, such as ZeXie Decoction and Shen Ling Bai Zhu San, which have all been applied to the treatment of several chronic illnesses in China [10,11]. *In vitro* experiments have also shown that the sesquiterpene compounds present in AM can protect the liver from damage [12] and that atractylode II and III may affect the farnesoid X receptor (FXR) [13] which is beneficial to the metabolism of cholesterol in the liver. It has been reported that AM contains many components, including volatile oils, sesquiterpenoids, and polysaccharides, among others, with the volatile oils and polysaccharides serving as its primary bioactive components [14]. However, as of yet, there has been no systematic study conducted to evaluate which of these components in AM may be used to treat hyperlipidemia effectively and safely, whether they affect HDL functionality, and what their mechanism are. Thus, the effect and mechanism of AM and its corresponding bioactive components on increasing HDL have important research significance and remain to be elucidated.

Given that TCM are synergistic, multi-target, and multi-component, the emerging tool that is network pharmacology has become a powerful aid to research [15]. Complex diseases like cardiovascular diseases rarely arise from single-molecule abnormalities or signaling pathway disorders, as such diseases are instead usually caused by the dysfunction of the regulation of a whole biological network. In contrast, network pharmacology can comprehensively reveal interactions between various disease and components targets [16]. TCM also takes a similar holistic approach to combating disease [17].

In the present study, the abilities of different AM extracts to elevate HDL and regulate blood lipid levels were evaluated and compared in hyperlipidemic rats. The network pharmacy analysis was then combined with experimental validation to study the bioactive components present in AM and their underlying mechanisms against hyperlipidemia. This research presents a novel medical foundation for the further advancement and application of AM in hyperlipidemia. The experimental flow chart is shown in Fig. 1.

2. Materials and methods

2.1. Chemicals and reagents

Enzyme-linked immunosorbent assay (ELISA) kits, including apolipoprotein B (Apo B), lecithin-cholesterol acyltransferase (LCAT), and apolipoprotein A1 (Apo-A1), were obtained from Shanghai Yuanye Biological Technology Co., Ltd. (Shanghai, China). Biochemical reagents including LDL-c, TG, HDL-c, TC, aspartate transaminase (AST), alanine transaminase (ALT), creatine (Cr), and blood urea nitrogen (BUN) were purchased from MeiKang Chemical Co. (Zhejiang, China). Hematoxylin and eosin (HE) kit were sourced from Nanjing Technology Co., Ltd. (Jiangsu, China). Antibodies against Apo-A1, GAPDH, and scavenger receptor type B I (SR-BI) were obtained from Hangzhou HuaAn Biotechnology Co., Ltd. (Zhejiang, China). LCAT was sourced from Proteintech (Chicago, USA). Rabbit and mouse-specific HRP/DAB (ABC) detection immunohistochemistry (IHC) kits were purchased from Abcam (Cambridge, USA).

AM was purchased from Panan County HSBC Chinese firms (Zhejiang, China). AM's standardization and identification were

according to the Chinese Pharmacopoeia (Commission of Chinese Pharmacopoeia, 2015). AM was identified by Professor Jingjing Yu (Zhejiang Chinese Medical University). Purified water was added to an alcoholic drink (52% alcohol (ethanol)), Erguotou, Red Star, Beijing, China) to reduce the alcohol content to 4%–22% (v/v). The Zhejiang Academy of Medical Science (Zhejiang, China) was the source of the basic diet supplies. High-sucrose, high-fat diet: consisting of 72.5% basic diet, 0.5% bile salt (w/w), 10% sucrose, 5% egg yolk powder, 10% lard, and 2 % cholesterol.

2.2. Animals

Eight-week-old (200 ± 20 g) female and male Sprague-Dawley (SD) rats ($n = 60$) were acquired from the Animal Supply Center of Zhejiang Academy of Medical Science (Zhejiang, China) under license number SCXK2008 0033. We employed a high-sucrose, high-fat diet, and alcohol (HSFDAC)-induced rats model of hyperlipidemia [18]. The humidity, temperature, and light/dark cycle of 12 h each day remained constant. All research conducted was adhered to the Guide for the Use and Care of Laboratory Animals published by the Zhejiang Province (2009).

2.3. Preparation of different extracts of AM

Water and petroleum ether, respectively, were used as solvents to extract AM to obtain AMW (water extract of AM) and AMO (petroleum ether extract of AM). The AMW was further alcohol precipitated, and the supernatant was AME (AM non-polysaccharides). Subsequently, the precipitate was diluted in distilled water to yield AMP (AM polysaccharides). The details of extraction procedure are shown in Fig. 2.

2.4. Treatment with different extracts of AM

Our previous study showed that SD rats could establish the hyperlipidemic models induced by the HSHFDAC [18]. The SD rats were categorized into six groups ($n = 10$, half male and half female). During the experiment, the normal group (NG) was given a basic diet and water. After four weeks of modeling, the HSHFDAC-induced hyperlipidemic rats were assigned to five groups by TC (G2, G3, G4, G5, and G6). And for the next four weeks, G2 rats (MG) were set as a model control group; G3, G4, G5, and G6 rats were given HSHFDAC and also, respectively, AMW (3500 mg/kg, p.o.), AMO (150 mg/kg, p.o.), AME (100 mg/kg, p.o.), or AMP (800 mg/kg, p.o.) according to body weight, once a day at the same time. The doses of all extracts from AM were the same, each of which was 10 g of crude AM per kilogram (kg) of rat weight.

Following an overnight fast, blood was collected from the ocular venous plexus of rats to measure levels of serum HDL-c, TC, and TG, which were determined using the appropriate kits by an automatic biochemical analyzer (TBA-40FR, TOSHIBA) at the time of the plan, as shown in the experimental outline. Serum LDL-c levels were subsequently calculated using Friedewald's formula. Based on the initial efficacy screening results, the optimal extract was selected. Throughout the experiment, food and caloric intakes, body weights, and blood glucose were evaluated.

2.5. Network pharmacology analysis

2.5.1. Screening of active compounds in AM

Based on the preliminary screening studies, AM's chemical components were searched using multiple databases, including China

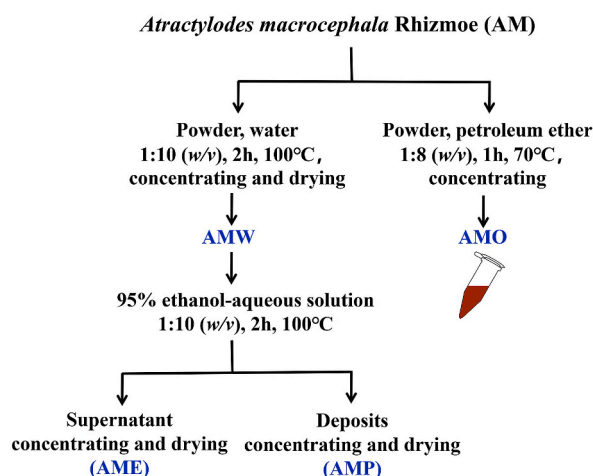


Fig. 2. Preparing different extracts of AM. AMW: The water extract of AM; AMO: The petroleum ether extract of AM obtaining AM oil; AME: AM non-polysaccharides. AMP: The deposits of AME obtaining AM polysaccharides.

National Knowledge Internet (CNKI: <http://www.cnki.net>), PubMed (<http://www.ncbi.nlm.nih.gov>), Wan Fang Database (<http://www.wanfangdata.com.cn/index.html>), and Traditional Chinese Medicine Systems Pharmacology Database and Analysis Platform (TCMSP, <http://tcmssp.com/index.php>). The 3D structure of the molecules was obtained by entering all AM compounds into both the TCMSP and PubChem databases.

Per DL (to predict drug-likeness) and Per OB (to predict oral bioavailability) were used to extract AM's active components after the TCMSP was used to assess the chemicals obtained above. Per DL ≥ 0.12 and Per OB $\geq 30\%$ were the two screening models' threshold values, respectively. Candidate active compounds were identified from the ensuing hits on active compounds.

2.5.2. Building an active compound-target network

Component targets were obtained through the TCMSP database, and gene names were obtained through the Uniports (<http://www.Uniprot.org/>) database. Compounds without targets and gene names were then eliminated. Importing candidate compounds and targets to the Cytoscape 3.7.0 software to build compound-target networks.

2.5.3. Predicting the hyperlipidemic targets

Four databases were searched in order to find the hyperlipidemic targets: the DisGeNET (<http://www.disgenet.org/>) database, the OMIM (<https://omim.org/>) database, the PHGKB (<https://phgkb.cdc.gov/PHGKB/startPagePhenoPedia.action/>) database, and the Genecards (<https://www.genecards.org/>) database. "Hyperlipidemia" or "HLP" as a keyword to search for hyperlipidemic targets. Screening for targets with relevance scores greater than 1 in the GeneCards database and target genes with gene-disease scores greater than 0.1 in the DisGeNET database. After eliminating duplicates, obtain the targets associated with hyperlipidemia.

2.5.4. Building networks for protein-protein interaction (PPI) and analyzing hub genes

The component targets of AM and the disease targets of hyperlipidemia were imported into an online website (<https://bioinfo.cnb.csic.es/tools/venny/index.html>) to plot a Venn diagram to obtain the common targets. To evaluate the protein interaction, the target genes in common were added to the STRING (<http://string-db.org/>) database. Then use Cytoscape to analyze the PPI network. The network nodes were analyzed using the "Network Analyzer". The degree is indicated by the color and size of the nodes, while the thickness of the edge indicates the "Combined Score" of the interaction. The Hub gene was then identified via the Cytohubba plugin for Cytoscape, utilizing the MCC method.

2.5.5. GO and KEGG analysis

We use the DAVID (DAVID, <https://david.ncicrf.gov/>) database to assess the Kyoto Encyclopedia of Genes and Genomes (KEGG) pathway enrichment and Gene Ontology (GO) function enrichment of the proteins in the PPI network.

2.5.6. Compounds-targets-pathways network building

Using Cytoscape, we built the "Compounds-targets-pathways (C-T-P)" network according to the findings of the KEGG analysis. The degree, which is a measurement of how many edges interact with nodes, was examined using Network Analyzer.

2.6. Experimental validation

2.6.1. Treatment with different doses of AMO

After treatment with different extracts of AM for four weeks, all the rats were discontinued for treatment but continued to be modeled with HSHFDAC for four weeks, except the normal group (NG; n = 10, half male and half female). Four weeks after the rats were modeled on HSHFDAC, they were randomly divided into four groups by TC (G2, G3, G4, and G5; n = 10, half female and half male). G2 rats (MG) were the model control group for the next four weeks; G3, G4, and G5 rats were given HSHFDAC and also, respectively, different doses of AMO (100 mg/kg, AMO-H; 50 mg/kg, AMO-M; and 25 mg/kg, AMO-L; p.o.) according to body weight once a day at the same time. Throughout the experiment, food and caloric intakes, body weights, and blood glucose were evaluated.

2.6.2. Determination of biochemical indicators

Serum HDL-c, TG, TC, BUN, ALT, Cr, and AST levels were measured with the appropriate kits. Serum LDL-c levels were calculated using Friedewald's formula.

2.6.3. Histopathology observation of liver and renal

Finally, the rats were euthanized under sodium pentobarbital anesthesia. Renal and liver tissues were fixed, dehydrated, embedded, and sectioned. As previously mentioned [19], all of the specimens were sliced using an LEICA RM2245 slicing machine (Germany) to a thickness of about 4 μm , and HE was used to stain them. The biological microscope BX43 (Olympus Optical Co., Ltd., Tokyo, Japan) was used for histopathology observation, and the analysis was done with Image-Pro Plus software.

2.6.4. Determination serum Apo-A1, Apo B, and LCAT activities

As directed by the manufacturer, the serum levels of Apo-A1, Apo B, and LCAT were detected with the ELISA kits.

2.6.5. SR-BI expression in liver with immunohistochemistry staining

As previously mentioned [19], after preventing and inactivating endogenous catalase, antigen retrieval, and reacting with the

primary antibody of SR-BI overnight (4 °C), a mouse and rabbit specific HRP/DAB (ABC) detection IHC kit was utilized for the reaction of SR-BI in paraffin liver sections. Sections were counterstained with DAB and hematoxylin. Under the biological microscope BX43 (Olympus Optical Co., Ltd., Tokyo, Japan), positive staining appeared yellow or brown. Protein levels were determined by measuring the integrated optical density in the positive area [20].

2.6.6. RT-PCR analysis of Apo-A1, LCAT, and SR-BI mRNA expression in liver

Using gene-specific primers, qRT-PCR was employed to examine the expression of Apo-A1, LCAT, SR-BI, and the reference gene GAPDH. We extracted the total RNA from the liver tissues. Afterwards, Superscript II qRT-PCR was used to extract the cDNAs. Primers specific for genes were utilized to amplify the RT product (1000 ng). The conditions for PCR were as follows: 94°C/2 min, 40 cycles of 94°C/15 s, 60°C/34 s. Threshold cycle (Ct) and melting curve calculations were performed. For quantitative analysis, the LightCycler 480 software was used by $2^{-\Delta\Delta Ct}$ [$\Delta Ct = Ct(\text{target}) - Ct(\text{GAPDH})$]. The primer information is presented in Table 1.

2.6.7. Western blot analysis of Apo-A1, LCAT, and SR-BI expression in liver

The frozen liver tissues were lysed for 30 min on ice in RAPI buffer containing protease/phosphatase inhibitors after being mechanically lysed in liquid nitrogen. After centrifuging the lysates for 15 min at 4 °C at 12,000 rpm, the bicinchoninic acid method was used to determine the protein content. SDS-PAGE was used to isolate the protein sample, which was then electrotransferred onto polyvinylidene difluoride membranes. GAPDH (Cat: ET1601-4) was the protein loading control. Membranes were cultivated with the related first antibody against Apo-A1 (Cat: ET1702-23), LCAT (Cat: 12243-1-AP), and SR-BI (Cat: ET1602-32) for a whole night at 4 °C. Membranes were washed three times with PBST before being cultivated with the relevant secondary antibodies (Cat: ab64264) for 2 h and then rinsed once more. The protein expression levels were standardized to GAPDH, and the blotted proteins were detected using a chemiluminescent assay kit.

2.7. Statistical analysis

The mean \pm standard deviation was used to express the measurement results. Statistical significance was defined as $P < 0.05$. Comparison between groups was made by applying SPSS 15.0 (SPSS Inc., Chicago, IL, USA) software. One-way analysis of variance was used to examine significant differences in the measurement traits, and either the Tukey honestly significant difference post hoc analysis or the Student's t-test analysis was employed after that.

3. Results

3.1. Effects of blood lipid with different extracts of AM

To investigate which bioactive components in AM may regulate blood lipid levels, we used HSHFDAC-induced hyperlipidemic rats to determine the effect of different extracts of AM on hyperlipidemia. Serum LDL-c and TC levels were significantly elevated compared with the NG ($P < 0.01$, Fig. 3A and C). The levels of serum HDL-c were significantly decreased in all groups after being fed with HSHFDAC for four weeks ($P < 0.01$, Fig. 3D), indicating successful modeling. After being fed with HSHFDAC for four weeks, the levels of serum TG showed no significant changes in all the groups (Fig. 3B). Compared with MG, only AMO significantly decreased serum LDL-c and TC levels and increased serum HDL-c levels in the HSHFDAC-induced hyperlipidemic rats compared with MG since the second week of treatment ($P < 0.01$, 0.05, Fig. 3A–C–D). The levels of serum HDL-c, LDL-c, and TC in rats after administration of AMW, AME, and AMP showed no significant changes compared with MG (Fig. 3A–C–D). Two weeks after AMO administration, serum LDL-c and TC levels in model rats began to decline significantly and steadily, and serum HDL-c levels significantly increased ($P < 0.01$, 0.05, Fig. 3A, C–D). During the four weeks of AMO administration, the above indicators remained stable. And there were no significant changes in caloric intake, body weights, or food intake in rats before and after administration of AMW, AME, and AMP compared with MG. After four weeks of administration, only AMO and AMP could significantly decrease blood glucose in the HSHFDAC-induced hyperlipidemic rats compared with MG (data not shown).

These results indicated that the AMO (volatile and liposoluble components) was the most effective in regulating blood lipid levels.

Table 1
Primer sequence of marker.

Genes	Sequences (5'–3')
LCAT	FORWARD: TGGCTTTGGCAAGACCTACTCTG REVERSE: TCTCATCCCGCACATACCCATTG
Apo-A1	FORWARD: GTGAAGATTTCGCCACTGTGTATG REVERSE: AGTTGTCCAGGAGATTGAGGTTTCAG
SR-BI	FORWARD: TTCTGGCGTCTTCACCGTCTTC REVERSE: GTTCCGAATGCCAATAGTTGACCTC
GAPDH	FORWARD: TGGCTTTGGCAAGACCTACTCTG REVERSE: TCTCATCCCGCACATACCCATTG

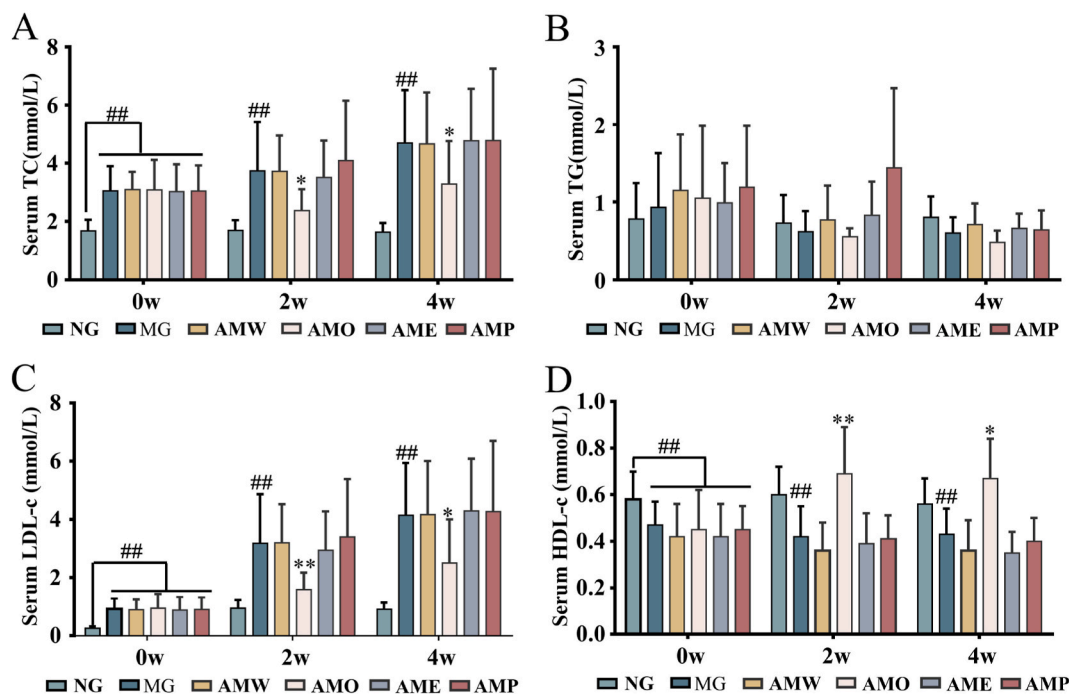


Fig. 3. Effects of blood lipid with different extracts of AM. A: Serum TC. B: Serum TG. C: Serum LDL-c. D: Serum HDL-c. AMW: The water extract of AM; AMO: The petroleum ether extract of AM obtaining AM oil; AME: AM non-polysaccharides. AMP: The deposits of AME obtaining AM polysaccharides. #*P* < 0.05, ##*P* < 0.01 vs. normal control, **P* < 0.05, ***P* < 0.01 vs. model group. *n* = 10.

3.2. Network pharmacology analysis

Pharmacodynamic preliminary screening results showed the AMO, which is mainly volatile and liposoluble, was the most effective in regulating blood lipid levels. Then network pharmacology was performed to explore the AM anti-hyperlipidemia's active compounds and potential mechanisms.

3.2.1. Screening for active compounds of AM

Approximately 131 components of AM were searched in multiple databases. The bioactive compounds were filtered based on parameters of ADME properties (Per DL \geq 0.12, Per OB \geq 30%). Eventually, 15 candidate compounds were selected, and the Per OB and Per DL of these active compounds varied from 33.94% to 68.11% and 0.12 to 0.78, respectively. Among them, atractylone, 3 β -acetoxyatractylone, atractylenolide iii, atractylenolide II, atractylenolide i, and so on are the primary components of AM's essential oil. The active compound information is presented in Table 2.

3.2.2. Compound-target (C-T) network analysis

The TCMSP database was searched for targets of compounds, and the Uniprot database was searched for gene names. Compounds without targets and gene names were then eliminated. As shown in Table 1S, we ultimately acquired 12 compounds and 90 candidate targets.

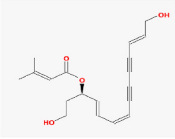
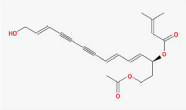
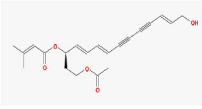
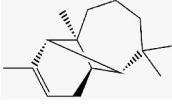
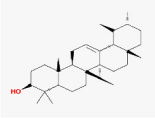
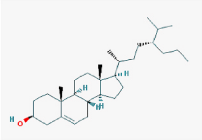
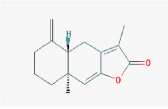
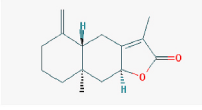
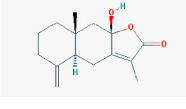
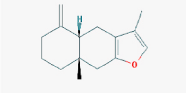
Import the components and component targets of AM into Cytoscape software to construct the Compound-Target network (C-T network). There were 280 edges and 102 nodes (12 bioactive compound nodes and 90 target nodes) in this network; volatile and liposoluble components such as atractylone (MOL000046, degree = 18) and 3 β -acetoxyatractylone (MOL000049, degree = 16) show a higher degree, indicating higher interaction with targets. As shown in Fig. 4.

3.2.3. Analysis hyperlipidemia of potential targets, PPI network, and hub gene

By searching the PHGKB, OMIM, DisGeNET, and Genecards databases, 545, 102, 69, and 802 hyperlipidemia disease-related targets were identified, respectively. After deleting duplicate targets, 1210 hyperlipidemia disease-related targets were obtained. The Venn diagram has 43 intersecting targets, indicating that the AM component targets share 43 common targets with hyperlipidemia (Fig. 5A).

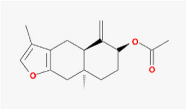
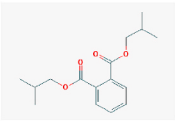
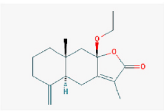
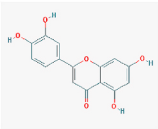
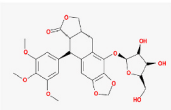
The PPI network is then built by uploading the common targets into the STRING database (PPI score >0.4) (Fig. 5B). The PPI network was analyzed using Cytoscape software, which has 282 edges and 43 nodes. Filtering Hub genes in this PPI network with Cytohubba. We identified the top 6 Hub genes of AM against hyperlipidemia using the MCC method (Fig. 5. C), which were vascular endothelial growth factor A (VEGFA), tumor necrosis factor (TNF), epidermal growth factor receptor (EGFR), RAC-alpha serine/

Table 2
Details about the 15 active compounds in AM.

Mol ID	Molecule Name	Structure	MW	OB (%)	DL
MOL000020	12-senecioidyl-2E,8E,10E-atractylentriol		312.39	62.4	0.22
MOL000021	14-acetyl-12-senecioidyl-2E,8E,10E-atractylentriol		355.44	60.31	0.31
MOL000022	14-acetyl-12-senecioidyl-2E,8Z,10E-atractylentriol		356.45	63.37	0.3
MOL000025	α -Longipinene		204.39	53.26	0.12
MOL000028	α -Amyrin		426.8	39.51	0.76
MOL000033	(3S,8S,9S,10R,13R,14S,17R)-10,13-dimethyl-17-[(2R,5S)-5-propan-2-yl-octan-2-yl]-2,3,4,7,8,9,11,12,14,15,16,17-dodecahydro-1H-cyclopenta[α]phenanthren-3-ol		428.82	36.23	0.78
MOL000043	Atractylenolide i		230.33	37.37	0.15
MOL000044	Atractylenolide II		232.35	47.5	0.15
MOL000045	Atractylenolide iii		248.35	68.11	0.17
MOL000046	Atractylone		216.35	41.1	0.13

(continued on next page)

Table 2 (continued)

Mol ID	Molecule Name	Structure	MW	OB (%)	DL
MOL000049	3 β -acetoxyatractylone		274.39	54.07	0.22
MOL000057	DIBP (diisobutyl phthalate)		278.38	49.63	0.13
MOL000072	8 β -ethoxy atractylenolide III		276.41	35.95	0.21
MOL000006	Luteolin		286.25	36.16	0.25
MOL001987	β -Sitosterol		546.57	33.94	0.7

Approximately 131 components of AM were searched in multiple databases, and 15 candidate compounds were selected based on the parameters of ADME properties (Per DL \geq 0.12, Per OB \geq 30%). ADME: Excretion, Absorption (OB), metabolism, and distribution (DL). MW: molecular weight.

threonine-protein kinase (Akt1), interleukin (IL)-6, and peroxisome proliferator-activated receptor gamma (PPARG). As shown in Table 3, the protein class of hub genes was analyzed through the DisGeNET database.

3.2.4. GO functional enrichment and KEGG pathway analysis

The molecular function, cellular component, and biological process of the 43 common targets were obtained by GO enrichment analysis. Fig. 6 lists these targets' top 10 significantly enriched GO terms (FDR<0.05). The results suggested that the common targets were strongly related to five biological processes: response to drug, positive regulation of nitric oxide biosynthetic process, positive regulation of transcription from RNA polymerase II promoter, positive regulation of protein phosphorylation, and positive regulation of cell proliferation (Fig. 6A); five cellular components: extracellular space, external side of the plasma membrane, plasma membrane, synapse, and integral components of the plasma membrane (Fig. 6B); and five molecular functions: cytokine activity, drug binding, enzyme binding, growth factor activity, and G-protein coupled acetylcholine receptor activity (Fig. 6C). As shown in Fig. 7, analysis of these targets' top 20 KEGG enriched gene pathways (FDR<0.05). According to the result, the targets were primarily linked with multiple signaling pathways, such as the phosphatidylinositol 3-kinase (PI3K)-Akt signaling pathway, the forkhead box O (FoxO) signaling pathway, regulation of lipolysis in adipocytes, non-alcoholic fatty liver disease, and insulin resistance.

3.2.5. Compound-target-pathway (C-T-P) network analysis

Using Cytoscape software to create "Compound-target-pathway (C-T-P)" networks (Fig. 8). Assembling the key pathways identified by analysis of the C-T-P network, volatile and liposoluble components, including atractylone (MOL000046, degree = 12) and 3 β -acetoxyatractylone (MOL000049, degree = 11), have a higher degree, which suggested that these volatile and liposoluble components are involved in relatively more interactions with various signaling pathways and targets, and so they could be the key compounds for AM in the therapy of hyperlipidemia. It was in agreement with the pharmacodynamic preliminary screening results. We identified five key signaling pathways that are strongly linked to AM treatment for hyperlipidemia by examining the C-T-P network. The five chosen pathways are: the PI3K-Akt signaling pathway (degree = 15), FoxO signaling pathway (degree = 9), non-alcoholic fatty liver disease (degree = 8), insulin resistance (degree = 7), and regulation of lipolysis in adipocytes (degree = 6).

3.3. Effects of blood lipid with different doses of AMO

Combining different AM extracts' preliminary pharmacodynamic experiments with network pharmacology analysis can verify that AMO treatment has the best improvement effect on regulating the level of blood lipids, especially increasing serum HDL-c levels. To

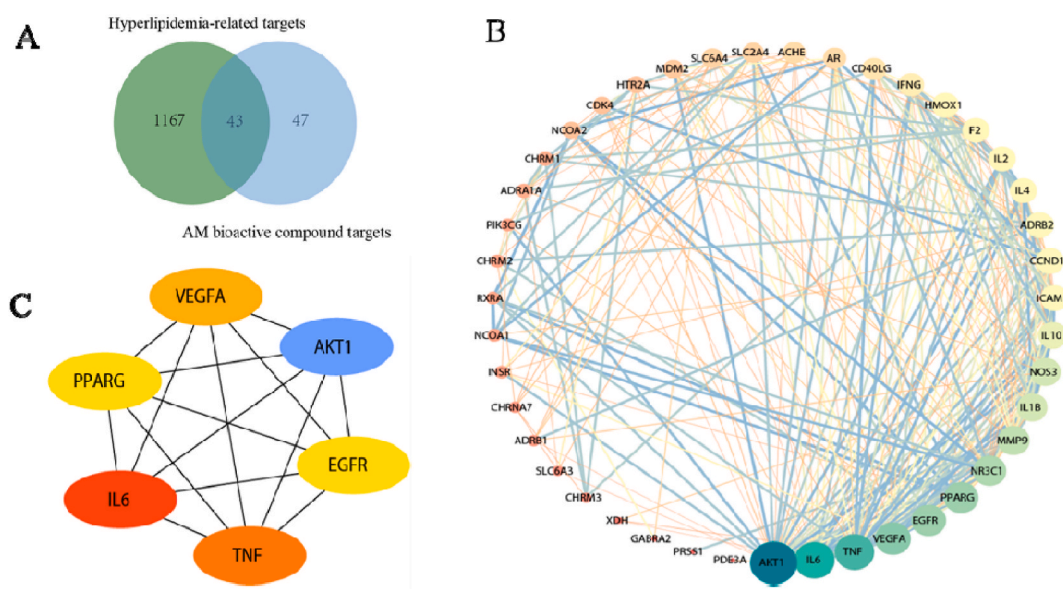


Fig. 5. Venn diagram of targets and protein-protein interaction (PPI) network of AM anti-hyperlipidemia. A: Venn diagram: the blue and green circles represent targets of AM and hyperlipidemia, respectively; B: PPI network (PPI score >0.4): the darker (greener) the color, the higher the degree, and the larger the nodes, the higher the degree. The combined score is represented by the edges; thicker edges indicate a higher score. C: Hub gene: Higher scores are obtained for nodes with darker (redder) colors. (For interpretation of the references to color in this figure legend, the reader is referred to the Web version of this article.)

Table 3

Details of selected the top six Hub genes.

Gene Name	Uniprot ID	Description	Protein Function
Akt1	P31749	threonine kinase 1/Akt serine/	RAS pathway related proteins; enzymes
IL6	P08887	Interleukin-6	A portion of the interleukin 6, activation results in immune response regulation
TNF	P01375	Tumor necrosis factor	TNFRSF1A/TNFR1 and TNFRSF1B/TNFR-binding; cytokine can cause specific tumor cell lines to die
VEGFA	P15692	vascular endothelial growth factor A	An essential component that controls adipose tissue angiogenesis
EGFR	P00533	Epidermal growth factor receptor	The process by which receptor tyrosine kinase binds EGF family ligands and initiates many signaling cascades to transform external signals into suitable cellular responses
PPARG	P37231	peroxisome proliferator activated receptor gamma	Nuclear receptors; Zinc-coordinating DNA-binding/Transcription factors AMmains

the hepatocyte membrane (the black arrow-yellow area represents SR-BI), and significantly decreased the expression levels of serum Apo B ($P < 0.05$, Fig. 10B), compared with MG; AMO-L significantly increased the expression levels of serum Apo-A1 ($P < 0.05$, Fig. 10A), and SR-BI in the hepatocyte membrane (Fig. 10D), and significantly decreased the expression levels of serum Apo B ($P < 0.05$, Fig. 10B), compared with MG.

Further, the results of Western blot and RT-PCR analysis showed that AMO significantly increased the expression of liver Apo-A1, LCAT, and SR-BI expression of protein (Fig. 10E–H), as well as the gene expression of them (Fig. 10I–K). It can be seen that the lipid-regulating effects of AMO may enhance serum HDL-c by increasing the expression of the RCT-related proteins Apo-A1, LCAT, and SR-BI.

3.5. Effects of renal and liver function with different doses of AMO

In this part, we evaluate the safety of AMO to raise HDL and regulate blood lipids by biochemical analysis, including levels of serum ALT, AST, BUN, uric acid (UA), and creatinine (Cr), and histopathological changes on the liver and kidney in the HSHFDAC-induced hyperlipidemic rats. After four weeks of treatment, AMO-H and AMO-M could significantly decrease levels of serum Cr ($P < 0.01$) (Fig. 11A), and all doses of AMO had no significant effect on other renal and liver injury biochemical indicators, including BUN, ALT, and AST (Fig. 11A and C).

Then, we carried out histological analysis of renal and liver sections with HE staining. As shown by the arrowheads, the HE staining revealed the presence of renal tubule dilatation, renal glomerular wall thickening, and inflammatory disorders in the renal (Fig. 11B)

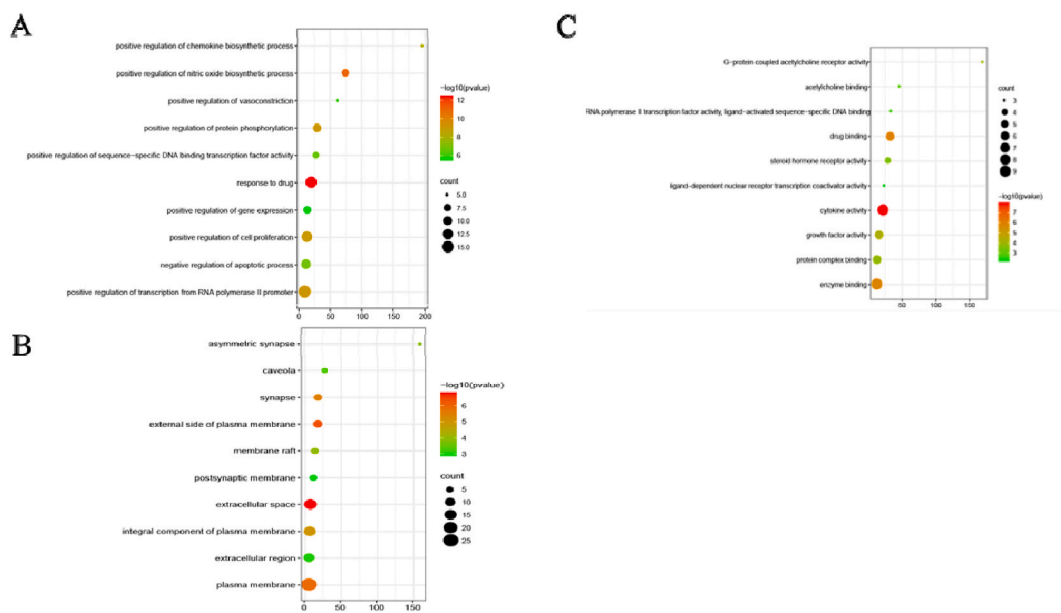


Fig. 6. GO functional enrichment analysis. A: Biological process enrichment, B: Cellular component enrichment, C: Molecular functions enrichment. The David database was used to analyze 43 common target genes of AM and hyperlipidemia. The first 10 results are shown in the figure.

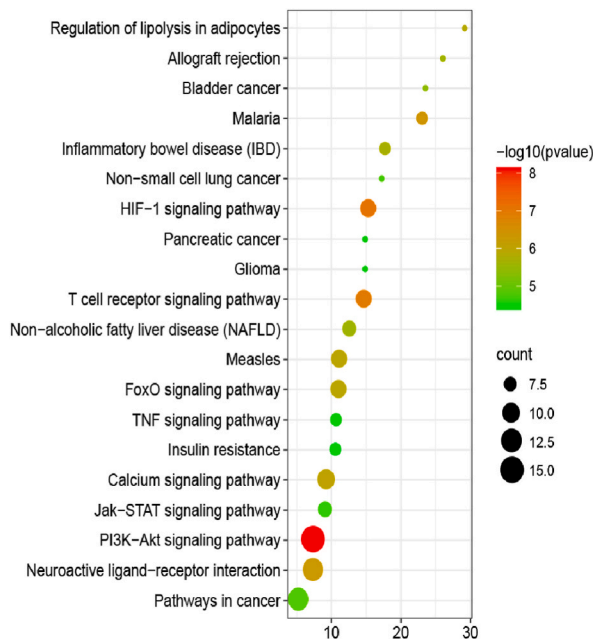


Fig. 7. KEGG pathway analysis. The David database was used to analyze 43 common target genes of AM and hyperlipidemia. The first 20 results are shown in the figure.

and hepatic steatosis with liver cell inflation reaction in the HSHFDAC-induced hyperlipidemic rats (Fig. 11D). After four weeks of AMO treatment, pathological changes were improved to varying degrees (Fig. 11B and D). It can be seen that the AMO significantly reduces serum Cr levels and improves histopathological changes in the liver and kidney. The results suggest that AMO elevated HDL and regulated lipid levels while having a better safety profile.

4. Discussion

Network pharmacology offers distinct benefits for finding drug targets and uncovering drug-target interactions [21]. The present

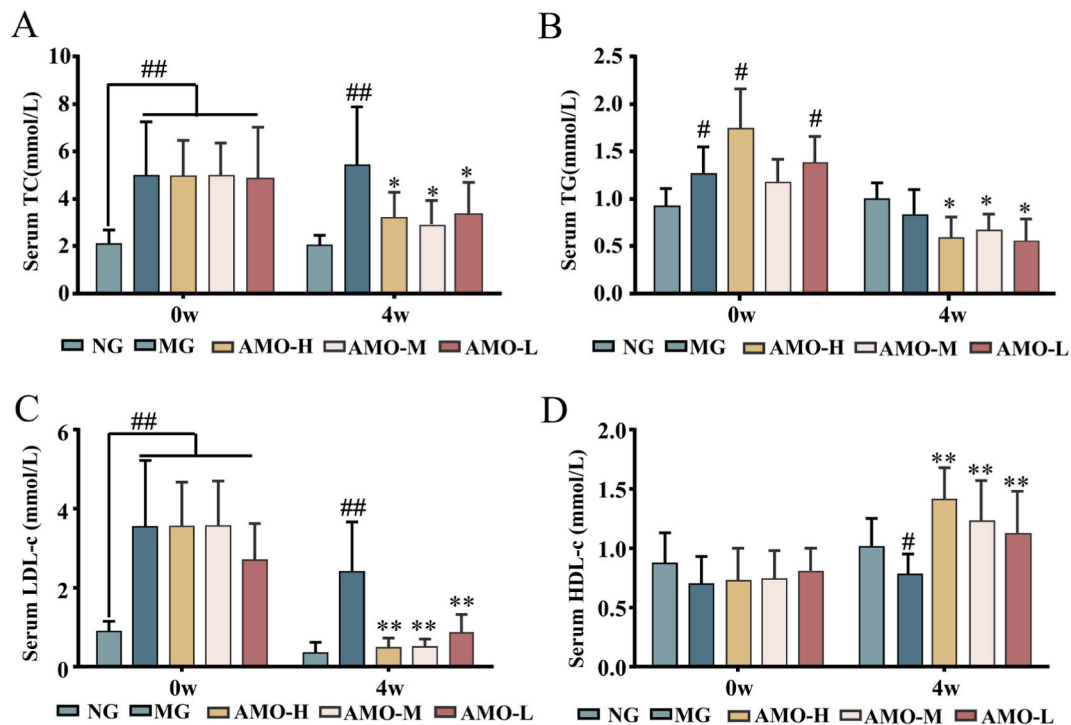


Fig. 9. Effects of blood lipids with three different doses of AMO. A: Serum TC. B: Serum TG. C: Serum LDL-c. D: Serum HDL-c. AMO: The petroleum ether extract of AM obtaining AM oil; AMO-H, -M, and -L respectively represented the high, medium, and low dose of AMO. # $P < 0.05$, ## $P < 0.01$ vs. normal control, * $P < 0.05$, ** $P < 0.01$ vs. model group. $n = 10$.

cholesterol [23]. Studies have shown that by modulating its downstream targets (the mechanistic target of rapamycin (mTOR) complex 1 (mTORC1), and hence the process of autophagy), Akt negatively regulates cholesterol efflux to Apo-A1 and thus affects the cholesterol level [24]. One study found that stimulating the adenosine 5'-monophosphate-activated protein kinase (AMPK)/Akt/mTOR signaling pathway might alleviate hyperlipidemia and hepatic steatosis [25]. Inflammation is linked with modifications in lipid metabolism that could be mediated by cytokines like TNF and IL-1. Inflammation promotes the secretion of TNF, which oxidizes LDL (ox-LDL) and promotes ox-LDL binding to the endothelial cells, increasing ox-LDL receptor expression [26]. Research has found that TNF- α prevents cholesterol efflux by mediating the overexpression of microRNA-101 and reducing the expression of ATP-binding cassette transporter A1 [27]. Conventionally, VEGF is thought to be important for angiogenesis and tissue remodeling. Nevertheless, recent research indicates that it also has potential roles in regulating energy metabolism, adipose tissue function, inflammation, and other biological activities [28,29]. PPAR γ , a nuclear receptor, is essential for regulating glucose and lipid homeostasis. Activating or inhibiting PPAR γ expression seems to alter most pro-adipogenic and anti-adipogenic regulators. These processes regulate the expression of adipocytokines and adipocyte-secreted proteins that promote lipid entry into the adipocyte, which decreases lipotoxicity [30,31].

The C-T-P network pharmacology analysis predicted that AM mediated several signaling pathways, with the PI3K signaling pathway possibly the principal one. Research indicates that the transcription factor FoxO1 and the production of fatty acids are both regulated by the PI3K/Akt/mTOR signaling pathway, which in turn regulates the metabolism of lipids [32]. Activating PI3K/Akt/mTOR/FoxO1 signaling induces decreased insulin resistance, thereby altering fat and glucose metabolism in diet-induced obesity [33]. On the one hand, Akt inhibition promotes ATP-binding-cassette A1 (ABCA1)-mediated cholesterol efflux to Apo-A1 by suppressing mTORC1. On the other hand, autophagy, which is one of the primary pathways of cholesterol transport, is increased upon Akt inhibition [23,24]. Moreover, Akt inhibition destabilizes lipid rafts, thereby promoting cholesterol efflux to Apo-A1 [34]. Therefore, via its downstream targets (including mTORC1, and, hence, the process of autophagy), Akt negatively regulates cholesterol efflux to Apo-A1.

RCT is the process by which HDL removes cholesterol from peripheral tissues, which is a crucial mode of lipid metabolism [35]. The primary extracellular carrier of cholesterol is HDL, which serves as the initial and speed-limiting stage in RCT [36]. Additionally, HDL maintains endothelium homeostasis and has antioxidant and anti-inflammatory properties [37]. Several plasma factors, such as Apo-A1, SR-BI, and LCAT, are participating in the RCT system, which can modulate HDL metabolism [38]. An epidemiological study has shown that baseline HDL-c efflux capacity is significantly associated with the incidence of cardiovascular disease events in the future [39]. Thus, therapeutically improving the functions of HDL, such as RCT and the elevation of HDL-c levels, is an essential method to treat hyperlipidemia. Apo-A1 is the most important apolipoprotein of HDL-c, and the contents of Apo-A1 are positively correlated with HDL-c. Apo-A1 performs a major housekeeping mechanism to support cellular cholesterol homeostasis. Apo-A1 can

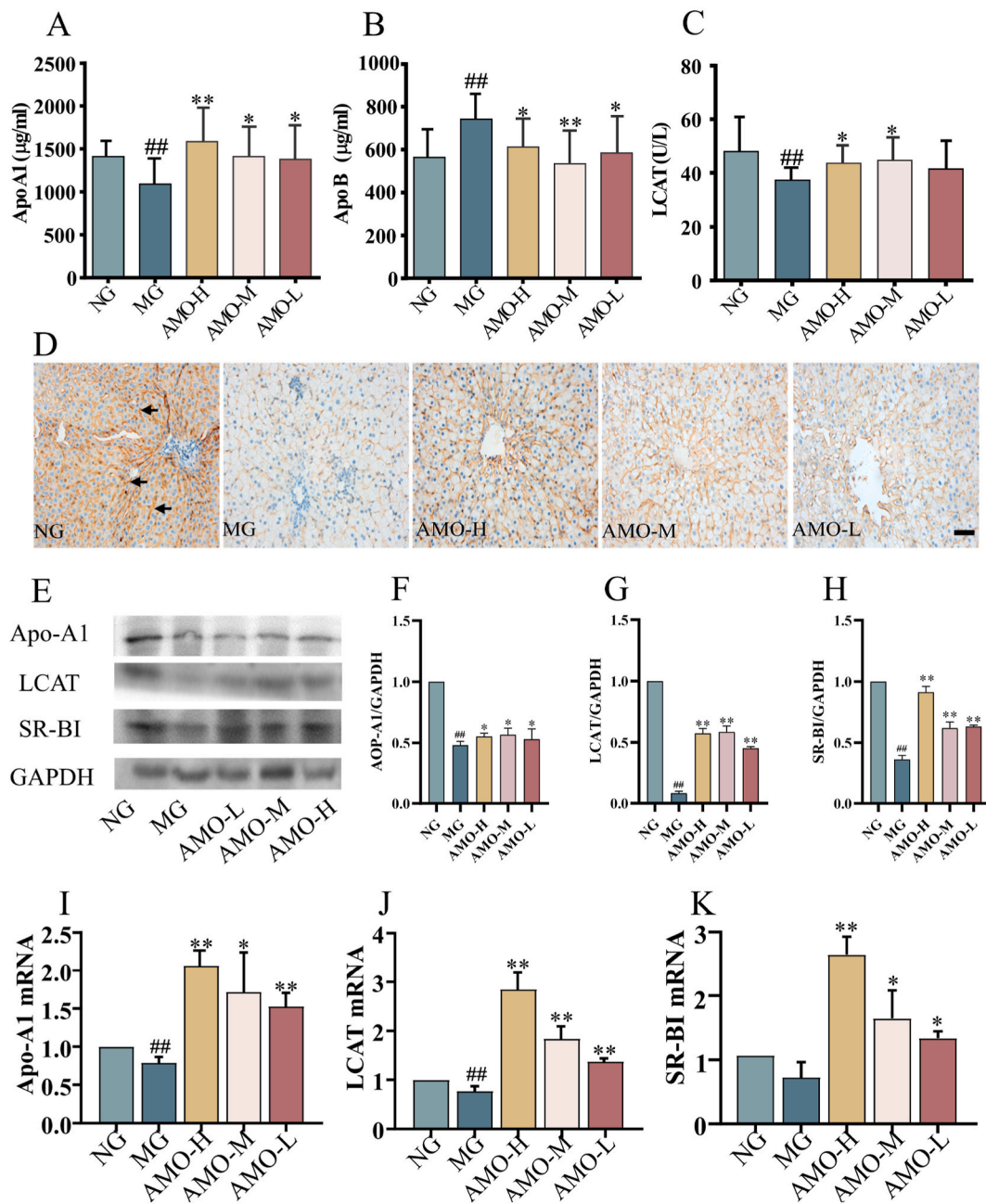


Fig. 10. Effects of Apo-A1, LCAT, and SR-BI expression with three different doses of AMO. A: Serum Apo-A1. B: Serum Apo B. C: Serum LCAT. D: Representative photomicrograph of SR-BI expression in hepatocyte membrane with immunohistochemistry staining (IHC, 400x; †: Representing positive expression). E-H: Representative Western blot analysis of the expression of Apo-A1, LCAT, and SR-BI (n = 3). For images of non-adjusted images blots are in the supplemental material (Fig. 1S). I-K: qRT-PCR analysis of Apo-A1, LCAT, and SR-BI mRNA expression (n = 3). AMO: The petroleum ether extract of AM obtaining AM oil; AMO-H, -M, and -L respectively represented the high, medium, and low dose of AMO. Scale bars, 120 μm #P < 0.05, ##P < 0.01 vs. normal control, *P < 0.05, **P < 0.01 vs. model group. A-D: n = 10.

promote cholesterol efflux from the peripheral tissues (like blood vessels, fat, and liver), which is then converted to immature HDL under the action of LCAT [40]. HDL-c in the blood passes through the SR-BI protein in the hepatocyte membrane and enters the liver to participate in its metabolic processes in a manner that is generally proportional to the level of serum HDL-c [41]. Several studies have shown that both hyperlipidemic patients and animal models of hyperlipidemia exhibit decreased expression levels of Apo-A1, LCAT, and SR-BI [40,41]. The current study found that AMO increased Apo-A1, LCAT, and SR-BI expression in hyperlipidemic rats. It has been suggested that AM may enhance the levels of serum HDL-c by increasing the expression of Apo-A1, LCAT, and SR-BI, and this effect is probably caused by their modulation of PI3K/Akt/mTOR&FoxO1 signaling. AM promotes cholesterol efflux to Apo-A1 by Akt

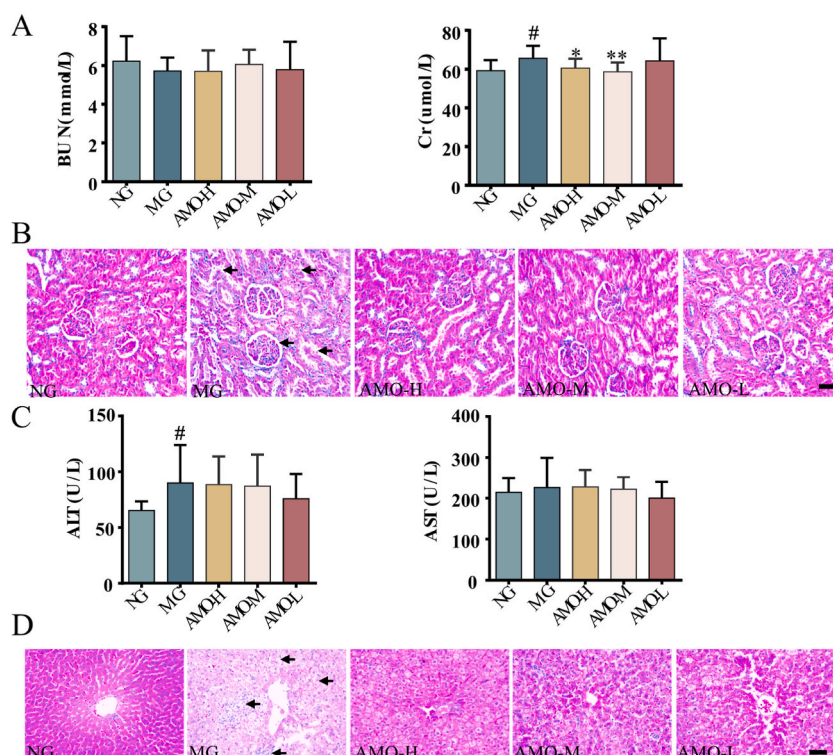


Fig. 11. Effects of renal and liver function with three different doses of AMO. A: Serum BUN and Cr biochemical index of renal function. B: Representative photomicrograph of histopathology observation of renal with HE staining (400x, †: Representing characteristic lesions). C: Serum ALT and AST biochemical index of liver function. D: Representative photomicrograph of histopathology observation of liver with HE staining (400x, †: Representing characteristic lesions). AMO: The petroleum ether extract of AM obtaining AM oil; AMO-H, -M, and -L respectively represented the high, medium, and low dose of AMO. Scale bars, 120 μm [#] $P < 0.05$, vs. normal control, ^{*} $P < 0.05$, ^{**} $P < 0.01$ vs. model group. $n = 10$.

inhibition, thereby enhancing serum HDL-c levels.

Liver and kidney function are important indicators for evaluating drug safety [42]. Therefore, it is important to determine the influence of AMO on liver and renal function. Following four weeks of treatment with different doses of AMO, the liver enzyme levels showed no significant change between the model and AMO-administered groups. However, the model group had extensive steatosis and some inflammation, according to the liver pathology results. The above pathologic changes were significantly improved in the AMO-administered groups. These findings suggested a discrepancy between pathological changes and serum transaminase levels. Our previous research revealed that *Dendrobii Officinalis* ultrafine powder improved liver hepatic steatosis and lipid deposition yet had no remarkable impact on serum transaminase levels, which may have something to do with the model group's normalization of these parameters [43]. Zhe Wu et al. [44] found that lipid vacuoles were observed in the hepatic tissue without significant changes in serum transaminase levels in mice fed a high-fat diet for eight weeks. We found that AMO improved hepatic steatosis and liver lipid accumulation, which showed that AMO might protect the liver and kidneys from damage. However, this study alone is insufficient for judging the toxicity of AMO. Our work simply suggests that the use of AMO at 25, 50, and 100 mg/kg dosages is not expected to cause liver or kidney damage.

Current niacin, fibrates, and statins are available to therapeutically elevate HDL-c [45]. Although statins are effective in lowering LDL-c levels, statins alone are usually not sufficient to increase HDL-c levels because of their slight effect on HDL-c levels (up to a 10% increase) [46]. Niacin has been shown to raise HDL-c by 20–30% [47], although 70% of subjects receiving niacin have been reported to have experienced flushes [48]. Fibrates may increase HDL-c (by approximately 10%) [49], but they also cause several adverse effects, including nephrotoxicity, liver toxicity, and rhabdomyolysis [50–52]. TCM have been extensively utilized as anti-hyperlipidemia agents; When compared to western drugs, they have fewer adverse effects and can be effective in the treatment of people with hyperlipidemia [53]. And the present study found that AMO can raise HDL-c by 200% and might protect the liver and kidneys from damage. Thus, AM could be developed as an efficacious and safe lipid-lowering drug.

There could be a few limitations on our research, though. To confirm the conclusions drawn from the results of the aforementioned studies, more biological studies are required. Moreover, we hope our study will help foster novel research to explore the utility of other Chinese herbs against hyperlipidemia.

5. Conclusion

In conclusion, the main bioactive compounds of AM that contribute to its anti-hyperlipidemia effect might include volatile and liposoluble components such as atractylone, which might enhance serum HDL-c levels by increasing the expression of Apo-A1, LCAT, and SR-BI. These components can significantly reduce serum Cr levels and improve histopathological changes in the liver and kidneys, which means that AM has a high safety profile for the liver and kidneys. This study will provide a novel scientific foundation for the application of AM to hyperlipidemia.

Funding

This work was supported by the Project of the National Natural Science Foundation of China, China (grant numbers 82003977, 82274134, 81803760 and 82274139), National Key Research and Development Plan, China (grant number 2017YFC1702200), and the Key Research and Development Program of Zhejiang Province, China (grant number 2020C04020).

Human and animal rights

All animal work was conducted according to the recommendations in the Guide for the Care and Use of Laboratory Animals of the National Institutes of Health. All procedures were performed according to protocols following the guidelines for the Use and Care of Laboratory Animals published by the Zhejiang province. And it was approved by the Ethics Committee.

Data availability statement

Data generated in this study are available from the corresponding author upon request.

CRediT authorship contribution statement

Bo Li: Writing – review & editing, Writing – original draft, Project administration, Methodology, Investigation, Formal analysis, Data curation, Conceptualization. **Xian-fang Chen:** Writing – review & editing, Writing – original draft, Visualization, Validation, Methodology, Investigation, Formal analysis. **Han-song Wu:** Writing – review & editing, Visualization, Validation, Software, Methodology, Investigation, Formal analysis. **Jie Su:** Writing – review & editing, Funding acquisition, Conceptualization. **Yan-yan Ding:** Methodology, Investigation. **Ze-hua Zhang:** Investigation. **Mei Rong:** Investigation. **Ying-jie Dong:** Writing – review & editing. **Xinglishang He:** Writing – review & editing. **Lin-zi Li:** Writing – review & editing. **Gui-yuan Lv:** Supervision, Project administration, Funding acquisition. **Su-hong Chen:** Supervision, Resources, Project administration, Funding acquisition.

Declaration of competing interest

The authors declare that they have no known competing financial interests or personal relationships that could have appeared to influence the work reported in this paper.

Acknowledgments

Not applicable.

Appendix A. Supplementary data

Supplementary data to this article can be found online at <https://doi.org/10.1016/j.heliyon.2024.e28019>.

References

- [1] W.H. El-Tantawy, A. Temraz, Natural products for controlling hyperlipidemia: review, Arch. Physiol. Biochem. 125 (2018) 128–135, <https://doi.org/10.1080/13813455.2018.1441315>.
- [2] L. Pan, Z. Yang, Y. Wu, R.X. Yin, Y. Liao, J. Wang, B. Gao, L. Zhang, The prevalence, awareness, treatment and control of dyslipidemia among adults in China, Atherosclerosis 248 (2016) 2–9, <https://doi.org/10.1016/j.atherosclerosis.2016.02.006>.
- [3] A. Alloubani, R. Nimer, R. Samara, Relationship between hyperlipidemia, cardiovascular disease and stroke: a systematic review, Curr. Cardiol. Rev. 17 (2021) e418418537, <https://doi.org/10.2174/1573403X16999201210200342>.
- [4] B. Gencer, N.A. Marston, K. Im, C.P. Cannon, P. Sever, A. Keech, E. Braunwald, R.P. Giugliano, M.S. Sabatine, Efficacy and safety of lowering LDL cholesterol in older patients: a systematic review and meta-analysis of randomised controlled trials, Lancet 396 (2020) 1637–1643, [https://doi.org/10.1016/S0140-6736\(20\)32332-1](https://doi.org/10.1016/S0140-6736(20)32332-1).
- [5] A.J. Gotto, J.E. Moon, Pharmacotherapies for lipid modification: beyond the statins, Nat. Rev. Cardiol. 10 (2013) 560–570, <https://doi.org/10.1038/nrcardio.2013.117>.

- [6] P. Barter, A.M. Gotto, J.C. LaRosa, J. Maroni, M. Szarek, S.M. Grundy, J.J. Kastelein, V. Bittner, J.C. Fruchart, HDL cholesterol, very low levels of LDL cholesterol, and cardiovascular events, *N. Engl. J. Med.* 357 (2007) 1301–1310, <https://doi.org/10.1056/NEJMoa064278>.
- [7] V.L. Roger, A.S. Go, D.M. Lloyd-Jones, E.J. Benjamin, J.D. Berry, W.B. Borden, D.M. Bravata, S. Dai, E.S. Ford, C.S. Fox, H.J. Fullerton, C. Gillespie, S. M. Hailpern, J.A. Heit, V.J. Howard, B.M. Kissela, S.J. Kittner, D.T. Lackland, J.H. Lichtman, L.D. Lisabeth, D.M. Makuc, G.M. Marcus, A. Marelli, D.B. Matchar, C.S. Moy, D. Mozaffarian, M.E. Mussolino, G. Nichol, N.P. Paynter, E.Z. Soliman, P.D. Sorlie, N. Sotodehnia, T.N. Turan, S.S. Virani, N.D. Wong, D. Woo, M. B. Turner, Executive summary: heart disease and stroke statistics—2012 update: a report from the American Heart Association, *Circulation* 125 (2012) 188–197, <https://doi.org/10.1161/CIR.0b013e3182456d46>.
- [8] J.S. Parham, A.C. Goldberg, Review of recent clinical trials and their impact on the treatment of hypercholesterolemia, *Prog. Cardiovasc. Dis.* 75 (2022) 90–96, <https://doi.org/10.1016/j.pcad.2022.11.011>.
- [9] A. Rauf, M. Akram, H. Anwar, M. Daniyal, N. Munir, S. Bawazeer, S. Bawazeer, M. Rebezov, A. Bouyahya, M.A. Shariati, M. Thiruvengadam, O. Sarsembenova, Y.N. Mabkhot, M.N. Islam, T.B. Emran, S. Hodak, G. Zengin, H. Khan, Therapeutic potential of herbal medicine for the management of hyperlipidemia: latest updates, *Environ. Sci. Pollut. Res. Int.* 29 (2022) 40281–40301, <https://doi.org/10.1007/s11356-022-19733-7>.
- [10] Q. Yang, Y. Xu, G. Feng, C. Hu, Y. Zhang, S. Cheng, Y. Wang, X. Gong, p38 MAPK signal pathway involved in anti-inflammatory effect of Chaihu-Shugan-San and Shen-ling-Bai-zhu-San on hepatocyte in non-alcoholic steatohepatitis rats, *Afr. J. Tradit., Complementary Altern. Med.* 11 (2014) 213–221, <https://doi.org/10.4314/ajtcam.v11i1.34>.
- [11] Y. Cao, J. Shi, L. Song, J. Xu, H. Lu, J. Sun, J. Hou, J. Chen, W. Wu, L. Gong, Multi-omics integration analysis identifies lipid disorder of a non-alcoholic fatty liver disease (NAFLD) mouse model improved by Zexie-Baizhu decoction, *Front. Pharmacol.* 13 (2022) 858795, <https://doi.org/10.3389/fphar.2022.858795>.
- [12] Y. Kiso, M. Tohkin, H. Hikino, Antihepatotoxic principles of *Attractylodes rhizomes*, *J. Nat. Prod.* 46 (1983) 651–654, <https://doi.org/10.1021/np50029a010>.
- [13] C. Tsai, J. Liang, H. Lin, Sesquiterpenoids from *Attractylodes macrocephala* act as farnesoid X receptor and progesterone receptor modulators, *Bioorg. Med. Chem. Lett.* 22 (2012) 2326–2329, <https://doi.org/10.1016/j.bmcl.2012.01.048>.
- [14] J. Zhang, G. Cao, Y. Xia, C. Wen, Y. Fan, Fast analysis of principal volatile compounds in crude and processed *Attractylodes macrocephala* by an automated static headspace gas chromatography-mass spectrometry, *Pharmacogn. Mag.* 10 (2014) 249–253, <https://doi.org/10.4103/0973-1296.137364>.
- [15] B. Boezio, K. Audouze, P. Ducrot, O. Taboureau, Network-based approaches in pharmacology, *Mol. Inform.* 36 (2017) 1700048, <https://doi.org/10.1002/minf.201700048>.
- [16] X.C. Pang, D. Kang, J.S. Fang, Y. Zhao, L.J. Xu, W.W. Lian, A.L. Liu, G.H. DU, Network pharmacology-based analysis of Chinese herbal Naodesheng formula for application to Alzheimer's disease, *Chin. J. Nat. Med.* 16 (2018) 53–62, [https://doi.org/10.1016/S1875-5364\(18\)30029-3](https://doi.org/10.1016/S1875-5364(18)30029-3).
- [17] T. Luo, Y. Lu, S. Yan, X. Xiao, X. Rong, J. Guo, Network pharmacology in research of Chinese medicine formula: methodology, application and prospective, *Chin. J. Integr. Med.* 26 (2020) 72–80, <https://doi.org/10.1007/s11655-019-3064-0>.
- [18] L.Z. Li, H.Y. Wang, J.H. Huang, K. Liu, X.J. Feng, X.M. Wang, L.J. Zhu, X.L. He, X. Zheng, H.L. Li, Y.J. Dong, B. Li, H.S. Wu, N.H. Jiang, G.Y. Lv, S.H. Chen, The mechanism of *Dendrobium officinale* as a treatment for hyperlipidemia based on network pharmacology and experimental validation, *Evid. Based. Complement. Alternat. Med.* 2022 (2022) 5821829, <https://doi.org/10.1155/2022/5821829>.
- [19] X. Chen, H.Z. Ge, S.S. Lei, Z.T. Jiang, J. Su, X. He, X. Zheng, H.Y. Wang, Q.X. Yu, B. Li, G.Y. Lv, S.H. Chen, *Dendrobium officinale* six nostrum ameliorates urate under-excretion and protects renal dysfunction in lipid emulsion-induced hyperuricemic rats, *Biomed. Pharmacother.* 132 (2020) 110765, <https://doi.org/10.1016/j.biopha.2020.110765>.
- [20] Y.J. Dong, N.H. Jiang, L.H. Zhan, X. Teng, X. Fang, M.Q. Lin, Z.Y. Xie, R. Luo, L.Z. Li, B. Li, B.B. Zhang, G.Y. Lv, S.H. Chen, Soporific effect of modified Suanzaoren Decoction on mice models of insomnia by regulating Orexin-A and HPA axis homeostasis, *Biomed. Pharmacother.* 143 (2021) 112141, <https://doi.org/10.1016/j.biopha.2021.112141>.
- [21] X. Wang, Z.Y. Wang, J.H. Zheng, S. Li, TCM network pharmacology: a new trend towards combining computational, experimental and clinical approaches, *Chin. J. Nat. Med.* 19 (2021) 1–11, [https://doi.org/10.1016/S1875-5364\(21\)60001-8](https://doi.org/10.1016/S1875-5364(21)60001-8).
- [22] G. Hoxhaj, B.D. Manning, The PI3K-AKT network at the interface of oncogenic signalling and cancer metabolism, *Nat. Rev. Cancer* 20 (2020) 74–88, <https://doi.org/10.1038/s41568-019-0216-7>.
- [23] R.M. Adam, N.K. Mukhopadhyay, J. Kim, D. Di Vizio, B. Cinar, K. Boucher, K.R. Solomon, M.R. Freeman, Cholesterol sensitivity of endogenous and myristoylated Akt, *Cancer Res.* 67 (2007) 6238–6246, <https://doi.org/10.1158/0008-5472.CAN-07-0288>.
- [24] P. Varshney, N. Saini, PI3K/AKT/mTOR activation and autophagy inhibition plays a key role in increased cholesterol during IL-17A mediated inflammatory response in psoriasis, *Biochim. Biophys. Acta, Mol. Basis Dis.* 1864 (2018) 1795–1803, <https://doi.org/10.1016/j.bbadis.2018.02.003>.
- [25] J. Zhong, W. Gong, L. Lu, J. Chen, Z. Lu, H. Li, W. Liu, Y. Liu, M. Wang, R. Hu, H. Long, L. Wei, Irbesartan ameliorates hyperlipidemia and liver steatosis in type 2 diabetic db/db mice via stimulating PPAR-gamma, AMPK/Akt/mTOR signaling and autophagy, *Int. Immunopharmacol.* 42 (2017) 176–184, <https://doi.org/10.1016/j.intimp.2016.11.015>.
- [26] L. Cominacini, A.F. Pasini, U. Garbin, A. Davoli, M.L. Tosetti, M. Campagnola, A. Rigoni, A.M. Pastorino, V. Lo Cascio, T. Sawamura, Oxidized low density lipoprotein (ox-LDL) binding to ox-LDL receptor-1 in endothelial cells induces the activation of NF-kappaB through an increased production of intracellular reactive oxygen species, *J. Biol. Chem.* 275 (2000) 12633–12638, <https://doi.org/10.1074/jbc.275.17.12633>.
- [27] N. Zhang, J. Lei, H. Lei, X. Ruan, Q. Liu, Y. Chen, W. Huang, MicroRNA-101 overexpression by IL-6 and TNF-alpha inhibits cholesterol efflux by suppressing ATP-binding cassette transporter A1 expression, *Exp. Cell Res.* 336 (2015) 33–42, <https://doi.org/10.1016/j.yexcr.2015.05.023>.
- [28] M. Shibuya, VEGF-VEGFR system as a target for suppressing inflammation and other diseases, *Endocr., Metab. Immune Disord.: Drug Targets* 15 (2015) 135–144, <https://doi.org/10.2174/1871530315666150316121956>.
- [29] I. Elias, S. Franckhauser, F. Bosch, New insights into adipose tissue VEGF-A actions in the control of obesity and insulin resistance, *Adipocyte* 2 (2013) 109–112, <https://doi.org/10.4161/adip.22880>.
- [30] R. Clasen, M. Schupp, A. Foryst-Ludwig, C. Sprang, M. Clemenz, M. Krikov, C. Thone-Reineke, T. Unger, U. Kintscher, PPARgamma-activating angiotensin type-1 receptor blockers induce adiponectin, *Hypertension* 46 (2005) 137–143, <https://doi.org/10.1161/01.HYP.0000168046.19884.6a>.
- [31] J. Ge, J.J. Miao, X.Y. Sun, J.Y. Yu, Huangkui capsule, an extract from *Abelmoschus manihot* (L.) medic, improves diabetic nephropathy via activating peroxisome proliferator-activated receptor (PPAR)-alpha/gamma and attenuating endoplasmic reticulum stress in rats, *J. Ethnopharmacol.* 189 (2016) 238–249, <https://doi.org/10.1016/j.jep.2016.05.033>.
- [32] Y. Jiao, X. Liang, J. Hou, Y. Aisa, H. Wu, Z. Zhang, N. Nuermaitaiti, Y. Zhao, S. Jiang, Y. Guan, Adenovirus type 36 regulates adipose stem cell differentiation and glucolipid metabolism through the PI3K/Akt/FoxO1/PPARgamma signaling pathway, *Lipids Health Dis.* 18 (2019) 70, <https://doi.org/10.1186/s12944-019-1004-9>.
- [33] L. Tang, C.T. Liu, X.D. Wang, K. Luo, D.D. Zhang, A.P. Chi, J. Zhang, L.J. Sun, A prepared anti-MSTN polyclonal antibody reverses insulin resistance of diet-induced obese rats via regulation of PI3K/Akt/mTOR&FoxO1 signal pathways, *Biotechnol. Lett.* 36 (2014) 2417–2423, <https://doi.org/10.1007/s10529-014-1617-z>.
- [34] E. Grao-Cruces, S. Lopez-Enriquez, M.E. Martin, L.P.S. Montserrat-de, High-density lipoproteins and immune response: a review, *Int. J. Biol. Macromol.* 195 (2022) 117–123, <https://doi.org/10.1016/j.ijbiomac.2021.12.009>.
- [35] S. Sacher, A. Mukherjee, A. Ray, Deciphering structural aspects of reverse cholesterol transport: mapping the knowns and unknowns, *Biol. Rev. Camb. Phil. Soc.* (2023), <https://doi.org/10.1111/brv.12948>.
- [36] A.D. Dergunov, V.B. Baserova, Different pathways of cellular cholesterol efflux, *Cell Biochem. Biophys.* 80 (2022) 471–481, <https://doi.org/10.1007/s12013-022-01081-5>.
- [37] A. Ossoli, C. Favero, L. Vigna, A.C. Pesatori, V. Bollati, M. Gomasarachi, Body mass index modulates the impact of short-term exposure to air particulate matter on high-density lipoprotein function, *Antioxidants* 11 (2022) 1938, <https://doi.org/10.3390/antiox11101938>.
- [38] D.E. Cohen, E.A. Fisher, Lipoprotein metabolism, dyslipidemia, and nonalcoholic fatty liver disease, *Semin. Liver Dis.* 33 (2013) 380–388, <https://doi.org/10.1055/s-0033-1358519>.

- [39] S. Ebtehaj, E.G. Gruppen, S. Bakker, R. Dullaart, U. Tietge, HDL (High-Density lipoprotein) cholesterol efflux capacity is associated with incident cardiovascular disease in the general population, *Arterioscler. Thromb. Vasc. Biol.* 39 (2019) 1874–1883, <https://doi.org/10.1161/ATVBAHA.119.312645>.
- [40] F. Oldoni, D. Baldassarre, S. Castelnuovo, A. Ossoli, M. Amato, J. van Capelleveen, G.K. Hovingh, E. De Groot, A. Bochem, S. Simonelli, S. Barbieri, F. Veglia, G. Franceschini, J.A. Kuivenhoven, A.G. Holleboom, L. Calabresi, Complete and partial lecithin: cholesterol acyltransferase deficiency is differentially associated with atherosclerosis, *Circulation* 138 (2018) 1000–1007, <https://doi.org/10.1161/CIRCULATIONAHA.118.034706>.
- [41] I. Muthuramu, R. Amin, J.P. Aboumsellem, M. Mishra, E.L. Robinson, B. De Geest, Hepatocyte-specific SR-BI gene transfer corrects cardiac dysfunction in scarb1-deficient mice and improves pressure overload-induced cardiomyopathy, *Arterioscler. Thromb. Vasc. Biol.* 38 (2018) 2028–2040, <https://doi.org/10.1161/ATVBAHA.118.310946>.
- [42] M. Ruscica, N. Ferri, R.D. Santos, C.R. Sirtori, A. Corsini, Lipid lowering drugs: present status and future developments, *Curr. Atherosclerosis Rep.* 23 (2021) 17, <https://doi.org/10.1007/s11883-021-00918-3>.
- [43] S. Lei, B. Li, Y. Chen, X. He, Y. Wang, H. Yu, F. Zhou, X. Zheng, X. Chen, N. Zhang, J. Sub, M. Yan, G. Lv, S. Chen, *Dendrobii Officinalis*, a traditional Chinese edible and officinal plant, accelerates liver recovery by regulating the gut-liver axis in NAFLD mice, *J. Funct. Foods* 61 (2019) 103458, <https://doi.org/10.1016/j.jff.2019.103458>.
- [44] Z. Wu, J. Tan, Y. Chi, F. Zhang, J. Xu, Y. Song, X. Cong, N. Wu, Y. Liu, Mesenteric adipose tissue contributes to intestinal barrier integrity and protects against nonalcoholic fatty liver disease in mice, *Am. J. Physiol. Gastrointest. Liver Physiol.* 315 (2018) G659–G670, <https://doi.org/10.1152/ajpgi.00079.2018>.
- [45] M.J. Chapman, W. Le Goff, M. Guerin, A. Kontush, Cholesteryl ester transfer protein: at the heart of the action of lipid-modulating therapy with statins, fibrates, niacin, and cholesteryl ester transfer protein inhibitors, *Eur. Heart J.* 31 (2010) 149–164, <https://doi.org/10.1093/eurheartj/ehp399>.
- [46] Y. Zhang, S. Luo, Y. Gao, W. Tong, S. Sun, High-density lipoprotein subfractions remodeling: a critical process for the treatment of atherosclerotic cardiovascular diseases, *Angiology* (2023) 1428926689, <https://doi.org/10.1177/00033197231157473>.
- [47] I.M. Singh, M.H. Shishehbor, B.J. Ansell, High-density lipoprotein as a therapeutic target: a systematic review, *JAMA* 298 (2007) 786–798, <https://doi.org/10.1001/jama.298.7.786>.
- [48] R.S. Birjmohun, B.A. Hutten, J.J. Kastelein, E.S. Stroes, Efficacy and safety of high-density lipoprotein cholesterol-increasing compounds: a meta-analysis of randomized controlled trials, *J. Am. Coll. Cardiol.* 45 (2005) 185–197, <https://doi.org/10.1016/j.jacc.2004.10.031>.
- [49] M. Gomaschi, M.P. Adorni, M. Banach, F. Bernini, G. Franceschini, L. Calabresi, Effects of established hypolipemic drugs on HDL concentration, subclass distribution, and function, *Handb. Exp. Pharmacol.* 224 (2015) 593–615, https://doi.org/10.1007/978-3-319-09665-0_19.
- [50] R.L. Attridge, C.R. Frei, L. Ryan, J. Koeller, W.D. Linn, Fenofibrate-associated nephrotoxicity: a review of current evidence, *Am. J. Health Syst. Pharm.* 70 (2013) 1219–1225, <https://doi.org/10.2146/ajhp120131>.
- [51] M. Florentin, E.N. Liberopoulos, D.P. Mikhailidis, M.S. Elisaf, Fibrate-associated adverse effects beyond muscle and liver toxicity, *Curr. Pharm. Des.* 14 (2008) 574–587, <https://doi.org/10.2174/138161208783885362>.
- [52] J. Wu, Y. Song, H. Li, J. Chen, Rhabdomyolysis associated with fibrate therapy: review of 76 published cases and a new case report, *Eur. J. Clin. Pharmacol.* 65 (2009) 1169–1174, <https://doi.org/10.1007/s00228-009-0723-7>.
- [53] A. Rauf, M. Akram, H. Anwar, M. Daniyal, N. Munir, S. Bawazeer, S. Bawazeer, M. Rebezov, A. Bouyahya, M.A. Shariati, M. Thiruvengadam, O. Sarsembenova, Y.N. Mabkhot, M.N. Islam, T.B. Emran, S. Hodak, G. Zengin, H. Khan, Therapeutic potential of herbal medicine for the management of hyperlipidemia: latest updates, *Environ. Sci. Pollut. Res. Int.* 29 (2022) 40281–40301, <https://doi.org/10.1007/s11356-022-19733-7>.